Received: 31 January 2019 | Revised: 29 July 2019 | Accepted: 17 August 2019 | Published on: 1 October 2019

DOI: 10.1002/met.1837

RESEARCH ARTICLE

Meteorological Applications RMetS

Major factors affecting the snow simulations by the JULES in New Zealand

Yang Yang | **Michael Uddstrom** | **Richard Turner** | **Mike Revell**

Meso-Scale Meteorology and Remote Sensing, National Institute of Water & Atmospheric Research (NIWA), Wellington, New Zealand

Correspondence
Yang Yang, Meso-Scale Meteorology and Remote Sensing, National Institute of Water and Atmospheric Research (NIWA), 301 Evans Bay Parade, Hataitai, Wellington, New Zealand.
Email: y.yang@niwa.co.nz, yang.yang816@gmail.com

Funding information
The National Institute of Water & Atmospheric Research (NIWA)

Abstract

Snow frequently occurs over New Zealand. The seasonal snow accumulation can be about 3 m deep in early spring at some locations. Thus, for numerical weather prediction and climate modelling over New Zealand, a reliable, sophisticated snow model that can properly describe the physical processes associated with snow cover is required. In the past, owing to a lack of snow observations, modelling and verification of snow processes was limited over New Zealand. In the present study, the multilayer snow scheme of the Joint UK Land Environment Simulator (JULES)—the land surface model used in New Zealand regional weather and climate models—was used to simulate the snow water equivalent (SWE) and snow density at two sites in the South Island of New Zealand. The model captured seasonal and interannual variability in snow accumulation and melt. However, large errors in the simulated SWE (up to 300 mm) were found during snowmelt periods and in relatively warm winters when a significant amount of liquid water was present in snow. Sensitivity tests showed that errors in the simulated long wave radiation (a negative bias of about 6 W/m^2), snow albedo (0.05–0.10) and air temperature for snow occurrence (T_c, about 0.5 K) were the major factors causing large errors in the simulated SWE. In addition, the simulated snow density was lower than observed. The relatively warm and humid maritime climate of New Zealand appears to make snow simulation in New Zealand more sensitive to long wave radiation, snow albedo and T_c than for continents.

KEYWORDS

calibration, forecasting, hydro-meteorology, modelling, sensitivity analysis, soil moisture

1 | INTRODUCTION

Snow on the ground is characterized by high albedo, low thermal conductivity and small roughness (e.g. Slater *et al*., 2001; Albert, 2002; Lemke *et al*., 2007). The snow cover, with its low thermal conductivity, acts like an insulator for the soil, preventing large air temperature changes (Stieglitz *et al*., 2003). Temporal and spatial variations in snow cover play an important role in the surface energy balance, as indicated by Arons and Colbeck (1995) and Gustafsson *et al*. (2001).

For numerical weather forecasting and climate modelling, hydrological forecasting and other applications, many snow schemes of varying complexity have been developed over the past decade (e.g., Vionnet *et al*., 2012). However, the representation of snow processes in all current land surface

models (LSMs) still show large deficiencies and need further improvements (Dirmeyer *et al*., 2006; Roesch, 2006; Feng *et al*., 2008; Rutter *et al*., 2009; Essery *et al*., 2013; Gunther *et al*., 2019). Specifically, large errors have been reported in the timing and amount of simulated snowmelt (Roesch, 2006; Feng *et al*., 2008). The performance of snow models differs for different environmental conditions for snow (Rutter *et al*., 2009). Calibration of snow models for a range of different environmental conditions is required to refine estimates of LSM parameters and is a very important part of snow model development.

New Zealand lies in the mid-latitudes of the southwest Pacific, surrounded by relatively warm seas. The Southern Alps form the backbone of South Island and receive a significant amount of snow each year (Figure 1). The seasonal snow accumulation in the early spring can be 3–4 m at some locations, for example, Mount Cook (Fitzharris and Garr, 1995; Fitzharris *et al*., 1999). In contrast to snow occurrence in most of the continents in the Northern Hemisphere, heavy snow frequently occurs over New Zealand mountains in humid maritime climate (Owens and Fitzharris, 2004). Precipitation may occur as rain and substantial snowmelt takes place at elevations of up to 2,500 masl in mid-winter, while snow may fall as low as to 500 masl in summer (Fitzharris *et al*., 1999). Jennings *et al*. (2018) analysed the rain–snow temperature threshold across the Northern Hemisphere and found that the air temperature at which rain and snow fall in equal frequency varies significantly, averaging 1.0°C and ranging from −0.4 to 2.4°C, and that continental areas generally exhibit warmer thresholds for snow, while maritime areas exhibit colder thresholds.

Snowmelt over New Zealand contributes up to 24% of the annual water inflows to major hydroelectricity lakes (McKerchar *et al*., 1998). Many New Zealand agriculture applications need the water from snowmelt for irrigation, so knowledge of snow accumulation is an important part of understanding the New Zealand economy. During the past decades, some research work has been conducted to understand the seasonal and interannual variability of snow cover. However, because of few snow observations, most of the research to understand the seasonal snow accumulation and interannual variability (Fitzharris and Garr, 1995; Clark *et al*., 2011), and the impact of climate change on seasonal snow has been based on snow modelling and simulations (Fitzharris *et al*., 1999). These snow models were simple conceptual models or temperature index snow models in which the physical processes associated with snowmelt and liquid water frozen, and the interaction of the snow cover and the underlying soil owing to exchange of heat and water, were not considered. In a study of the sensitivity of parameters in snow simulation, Etchevers *et al.* (2004) indicated that a neglect of internal snowpack processes leads to deficiencies in snow simulation. In addition, verification of the snow models in these studies was more qualitive than quantitive owing to a lack of observations. Snow simulation over New Zealand using a more sophisticated snow model was also conducted by Clark *et al*. (2011). For hydrological application, the present study focused on the spatial variations of snow in a catchment and the key processes that affected the spatial variations of snow, not the model's performance in the simulation of snow depth at specific locations. The key factors affecting snow simulations in New Zealand are still not well known despite the studies mentioned above.

For numerical weather prediction and climate modelling, the snow model needs to represent properly the effects of snow on albedo and the heat and moisture exchange between snow surface and the atmosphere. The snow scheme of the Joint UK Land Environment Simulator (JULES) (Best *et al*., 2011) was developed for this purpose. JULES, a state-of-the-art LSM, was based on the Met Office's Surface Exchange Scheme (MOSES) (Cox *et al*., 1999). MOSES was a participant model in the Snow Model Intercomparison Project (SNOWMIP2) (Essery *et al*., 2009; Rutter *et al*., 2009). The snow scheme used in the MOSES and later in the JULES has undergone several improvements. The most recent is the introduction of the multilayer snow model in which snow is allowed to hold some liquid water (Best *et al*., 2011). Using snow depth observations from Austria, Parajka *et al*. (2010) verified the simulated snow cover and depth by the single-layer snow scheme of the JULES. They showed good agreement between simulations and observations in snow cover, but much larger differences in snow depth and poor performance of snow depth simulation in regions of significant topographical heterogeneity. In a recent evaluation of the JULES multilayer snow scheme in Norway, Vikhamar-Schuler *et al*. (2012) showed that the simulated snow depth was improved by modifying the fresh snow density (from 250 to 100 kg/m^3) and fresh snow albedos (from 0.98 to 0.8 for visible and from 0.7 to 0.5 for near infrared). JULES is the key LSM coupled with the Met Office's Unified Model (UM). The New Zealand Limited Area Model (NZLAM) (Yang *et al*., 2011, 2012), the New Zealand Convective Scale Model (Yang *et al*., 2017) and the New Zealand regional climate model are all configurations of the UM. Thus, it is necessary to understand the performance of the JULES in snow simulations over New Zealand in order to understand better and improve the performance of these local configurations.

The objective of the present study is to verify the snow water equivalent (SWE, mm), and snow density simulated by the standalone JULES multilayer snow scheme in New Zealand conditions, and to conduct sensitivity tests to understand the major factors and parameters that lead to the

large errors in the SWE and snow density. The paper is structured as follows. A short description of the JULES and the multilayer snow scheme is given in Section 2. A description of snow observations at two sites in New Zealand and an analysis of the data quality are given at Section 3. Verification of the simulated SWE and snow density is described in Section 4. Sensitivity tests for snow simulation are analysed in Section 5. Finally, conclusions and a discussion are given in Sections 6 and 7, respectively.

2 | A DESCRIPTION OF THE MODEL

The multilayer snow scheme (Best *et al*., 2011) of the JULES (v3.1) was used in the present study. One advantage of the JULES multilayer snow model is that it considers the snow liquid water. This relieved the problem of snowmelting too rapidly that was found in the zero-layer snow scheme of JULES (Best *et al*., 2011). Another advantage of the multilayer snow scheme of the JULES is that snow density is a prognostic variable. Essery *et al*. (2013) showed that the best simulations were found for models with prognostic snow albedo and density.

The data driving the model include air temperature, humidity, wind, pressure, precipitation and downward shortwave radiation (SW), and downward long wave radiation (LW). A maximum of seven snow layers were set with layer thicknesses of 0.1, 0.2, 0.3, 0.4, 0.5, 0.6 and 0.7 m, respectively.[1] The snow depth determines the number of layers actually used in the model. The bottom layer of the snowpack has a variable thickness. Precipitation is treated as either snow or liquid water depending on whether or not the 1.5 m air temperature for snow (T_a) exceeds a threshold (T_c), which is typically specified to be 274 K (the default value) in the JULES. The sensitivity of the SWE to T_c is reported in Section 5.4.

The change of snow mass in a layer is calculated using the difference in the snow temperature and the melting point temperature for water. The variation of the snow temperature is determined by the net heat flux in the layer along the vertical direction. For the top snow layer, the snow surface temperature T_* is calculated following Best *et al*. (2011) using:

$$C_1\frac{\delta T_*}{\delta t}=(1-\alpha)\mathrm{SW}\downarrow+\epsilon\mathrm{LW}\downarrow-\epsilon\sigma T_*^4-H-E-G_0 \quad (1)$$

where C_1 is the snow heat capacity (J/K) of the top snow layer; δt is a time step; α is the snow albedo; ϵ is the snow surface emissivity; σ *is the* Stefan Boltzmann constant ($5.67\times10^{-8}kgs^{-3}K^{-4}$); H is the sensible heat flux; E is the latent heat flux (W/m^2); SW$\downarrow$ is the downward SW; LW$\downarrow$ is the downward LW (W/m^2); and G_0 is the heat flux into the deeper snow layer.

For a given snow mass, the depth of snow is determined by snow density. The increase of snow density in snow layer k due to compaction over a time step is calculated as (Best *et al*., 2011):

$$\frac{\delta\rho_k}{\delta t}=\frac{\rho_k g M_k}{\eta}\exp\left(\frac{k_s}{T_m}-\frac{k_s}{T_k}-\frac{\rho_k}{\rho_0}\right) \quad (2)$$

where M_k is the snow mass above the middle of the snow layer k. For a snow temperature (T_k) range of 268–273 K, with ρ_0 about 50 kg/m^3 and compactive viscosity η between 5×10^6 and 14×10^6 Pa s, k_s has a valid range between 2,600 and 4,600 K. T_m is the freezing point of water and is 273.15 K. k_s and η are typically set to be 4,000 K and 1×10^7 Pa s, respectively. Sensitivity tests of the SWE to η are reported in Section 5.3. This scheme is based on Kojima (1966) and has been used in some previous snow models (e.g., Pitman *et al*., 1991; Lynch-Stieglitz, 1994).

Snow layers are allowed to retain a maximum liquid water content of 0.05 as a fraction of snow volume. When the liquid content of a layer exceeds this capacity, excess water is passed down to the layer below. The water flux at the base of the snowpack is passed to the surface hydrology module. Runoff occurs when the water flux at the base of the snowpack exceeds the water flux into the soil. For a snow simulation at a site by the JULES, blowing snow was not considered, but this will be included in future (Best *et al*., 2011, has a more detailed description of the model).

3 | DATA AND METHOD

Routine hourly snow depth observations have been collected since 2008 at nine sites in mountain areas over the South Island of New Zealand (Figure 1). Hourly SWE are available at half these sites, and some surface meteorological observations are also available at the nine sites. However, to meet the input data requirements of the JULES and to verify the simulated SWE and density, only two of the nine sites have suitable measurements. No sites measured LW, so LW simulated by the NZLAM was used to fill the data gap. Comparisons of the NZLAM LW estimates with observations made during the Deep Propagating Gravity Wave Experiment over New Zealand, June–July 2014 (DEEPWAVE) (Fritts *et al*., 2015) are presented and the sensitivity of snow simulation to LW are conducted in Section 5.1.

The two sites, Mueller Hut and Mahanga on the South Island, are about 2 km asl (Figure 1) and found within terrain that consists of bare soil and rocks with some short grass (0.05 m high, < 10% coverage) in summer. The vegetation was kept the same for the snow simulations (i.e. the dynamic vegetation model within the JULES was not used). The soil parameters were derived from the ancillary files of

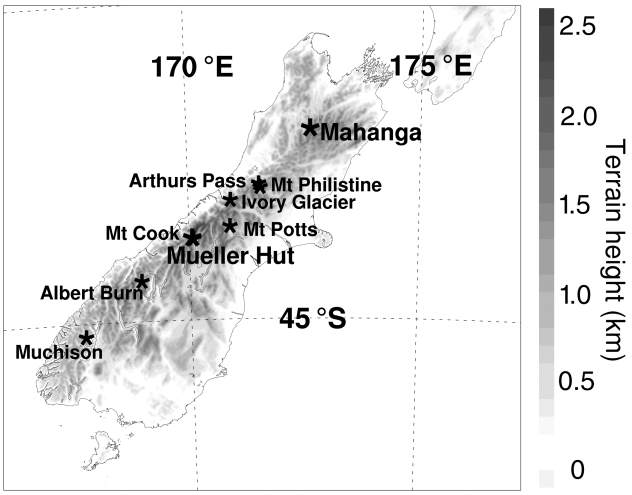

FIGURE 1 Locations (star signs) of the sites with snow observations over the South Island of New Zealand. Mueller Hut and Mt Cook are very close. Arthurs Pass and Mt Philistine are very close. Only observations from Mahanga and Mueller Hut were used in the present study. See the text for more information

the UK Met Office's UM model (Webster *et al*., 2003; Walters *et al*., 2011). While some failures of the snow sensor for snow depth and SWE did occur, especially at Mahanga, the data had sufficient temporal coverage for the purposes here.

Figure 2 shows the relationship between the hourly SWE and snow depth observations. The SWE is a measurement of the weight/pressure of the snowpack from a snow pillow by UNIK5000. The snow depth is measured by Campbell SR50A (with a sensor grill 3.84 m above the ground). The SWE and snow depth data used in the present study were quality checked. The thick straight solid lines in Figure 2 denote the linear regression between snow depth and SWE with the slope close to the overall mean snow density for all the available time. The slopes are 0.44 (440 kg/m^3) and 0.43 (430 kg/m^3) at Mueller Hut (Figure 2a) and Mahanga (Figure 2b), respectively. A notable feature for both sites is that more points lie above the regression lines for deeper snow, while more points lie below the regression solid lines for shallower snow, indicating that snow density tends to increase as the snow depth increases, consistent with what occurs in reality. The correlation between the SWE and snow depth is 0.98 at Mueller Hut and 0.97 at Mahanga. These facts indicate the overall reliability of the snow observation data. However, many points are also above the solid line with a snow depth about ≤ 200 mm at Mueller Hut (Figure 2a) and about ≤ 100 mm at Mahanga (Figure 2b). These cases mainly occurred at the last stage of snowmelt when snow depth was very shallow and much liquid water was still stored in the shallow snow. This could lead to a quite large snow density that was much greater than the average density (the solid line). However, this may also have resulted from the errors of the snow depth sensor and the SWE measuring equipment for very shallow snow. A smaller error in snow depth and/or in the SWE for shallow snow could lead to larger errors in density. To avoid this complication, in the following verification of snow density, the periods of snowmelt were excluded when snow depth was ≤ 100 mm. In addition, many points are also found below the solid straight line for snow depth > 2.0 m at Mueller Hut and > 0.6 m at Mahanga. These cases occurred when a significant fraction of the snow was fresh with much lower density.

At the two sites, the rain gauges had no heating device and could not measure solid precipitation (snow/ice). Figure 3 shows the air temperature and hourly precipitation at the two sites. The precipitation during freezing weather was not well recorded. A dramatic change in hourly rainfall amount was found at 0°C at both stations (Figure 2a,c).

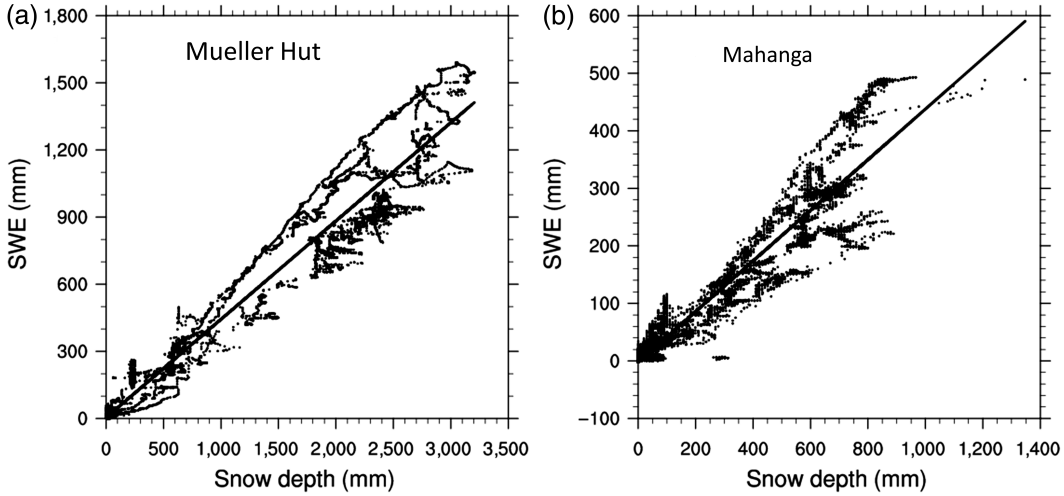

FIGURE 2 Scatter plots of hourly snow water equivalent (SWE) and snow depth at (a) Mueller Hut (38102) and (b) Mahanga (36857) in New Zealand. The thick straight solid lines denote the linear regression and the slope corresponding to an average snow density of about 440 kg/m^3 at Mueller Hut and about 430 kg/m^3 at Mahanga

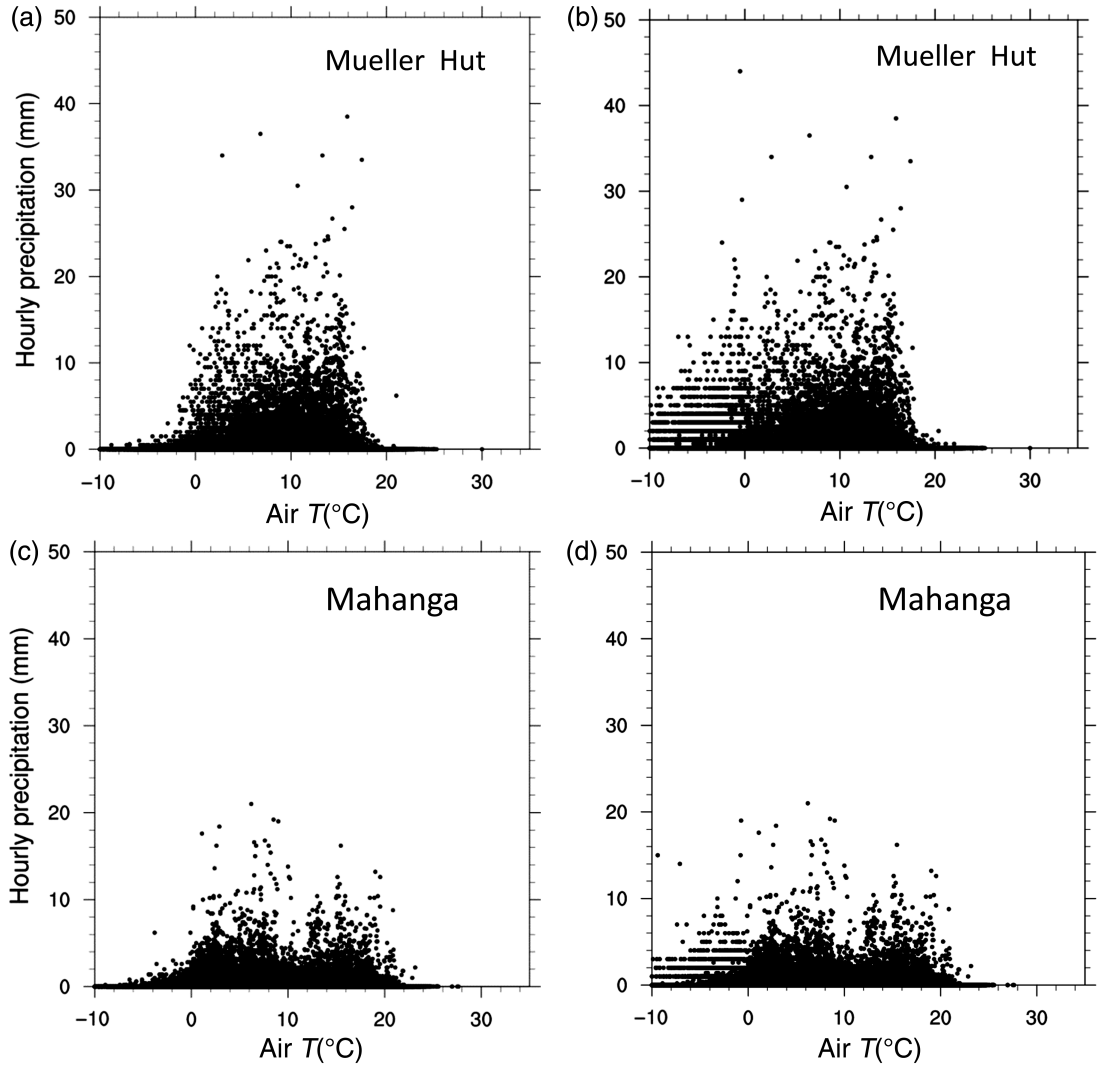

FIGURE 3 Scatter plots of hourly air temperature at the surface and the original hourly precipitation at (a) Mueller Hut and (c) Mahanga, and the hourly air temperature at the surface and the regenerated hourly precipitation using the snow water equivalent (SWE) and the original precipitation at (b) Mueller Hut and (d) Mahanga

Using the rain gauge observations only, the simulated SWE was < 10% of the observations at the two sites. The observed SWE was therefore used to recover the missing precipitation during freezing weather. When the air temperature was < 0.0°C, the SWE increment was then taken as the missing precipitation. This procedure, together with the 1 mm precision of the SWE measurements, produced the horizontal lines seen in Figure 3b,d for air temperature < 0°C.

Fresh snow density needs to be specified for the JULES; the default is 100 kg/m^3. At the two sites, fresh snow density can be calculated using the hourly increment of snow depth and snowmass. For all available snow observations used in the present study, the fresh snow density ranged from about 50 to about 200 kg/m^3, and the mean and median were about 105.0 and about 96.0 kg/m^3, respectively. Thus, a fresh snow density of 100 kg/m^3 was used.

Hourly data were available to run the JULES from 13 April 2010 to 1 September 2012 at Mueller Hut, and from 1 April 2009 to 1 September 2011 at Mahanga. The JULES needs a spin-up period to generate realistic soil moisture and soil temperature. Following Yang *et al.* (2013), the first year's data at each site were used to spin-up the JULES. To decide whether adequate spin-up had occurred, it was required that the differences in soil temperature and soil moisture at each soil layer between two consecutive cycles be < 0.5 K and 0.5 mm, respectively. Once these conditions were met, model outputs were used for analysis.

4 | VERIFICATION

To reduce the effect of random errors in the hourly SWE and snow depth observations on verification of the simulated

SWE and snow density, daily mean (calculated from the hourly observations) SWE and snow density were used.

4.1 | Snow water equivalent (SWE)

Figures 4 and 5 show the simulated SWE at the two sites. Because some snow observations were missing due to sensor failure, snow simulation results were not shown before 1 July 2011 (Figure 4c) at Mueller Hut. Most of the SWE and snow depth observations at Mahanga in 2011 were missing due to sensor failure. Generally, for the control simulation with default settings in the JULES (CTRL) (Table 1), the simulated SWE was close to observations of snow accumulation and snowmelt at the two sites (Figures 4 and 5). In simulations and observations the time of maximum snow accumulation (in mid-spring) matched very well. However, there were some instances of large errors in the amount of the simulated SWE.

At Mueller Hut in 2010 (Figure 4a) and 2012 (Figure 4c), the simulated SWE was generally greater ($\leq$ 300 mm) with a later end of the snow season than was observed. In 2010, some snow accumulation was observed from the end of April to the beginning of May, but it melted completely before 20 May (Figure 4a). The observed snow accumulation actually started at the end of May. In contrast, the simulated snow accumulation started at the end of April and lasted until the end of December. There was much more simulated snow than was observed from the end of April to the end of May. The simulated snow for this period only partly melted. Furthermore, in July, the observed SWE varied little whereas the simulated SWE showed a significant increase with time. This led to a large difference between observations and simulations in July (Figure 4a). The relatively large errors in the simulated SWE during these two time periods contributed significantly to the errors after July in 2010.

At Mahanga in 2009 (Figure 5a) the simulated SWE was greater ($\leq$ 300 mm) than that observed, and had a later snow termination. In 2010 (Figure 5b), the simulated snow started and terminated later than that observed, and the simulated SWE was slightly less than that observed during the snow accumulation period and greater ($\leq$ 100 mm) during snowmelt.

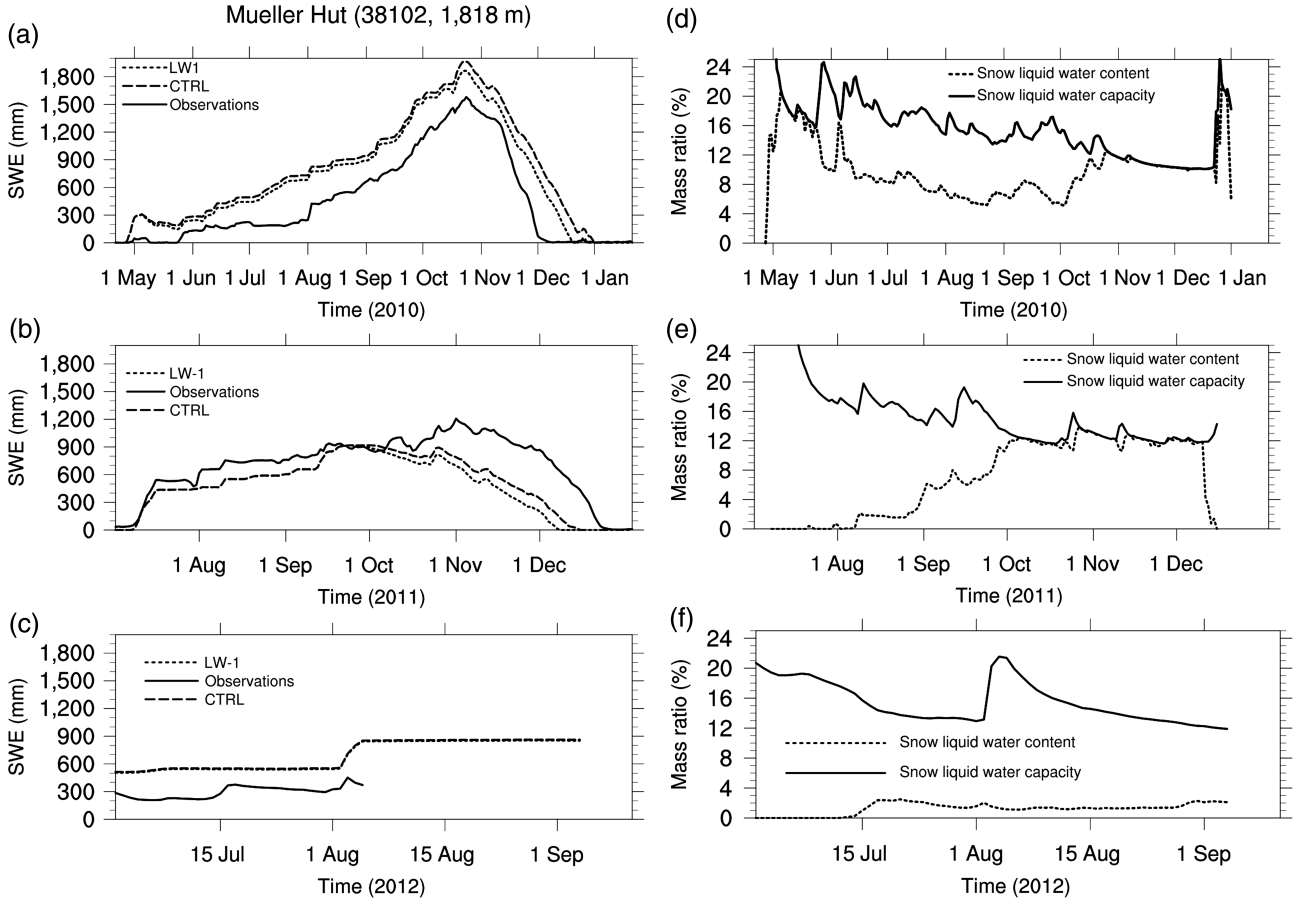

FIGURE 4 Simulated and observed snow water equivalent (SWE) at Mueller Hut in (a) 2010, (b) 2011 and (c) 2012. Snow liquid water content and snow liquid water capacity (SLWC) for the CTRL at Mueller Hut in (d) 2010, (e) 2011 and (f) 2012. The downward long wave radiation (LW-1) is the sensitivity test of the LW, as described in Section 5.1

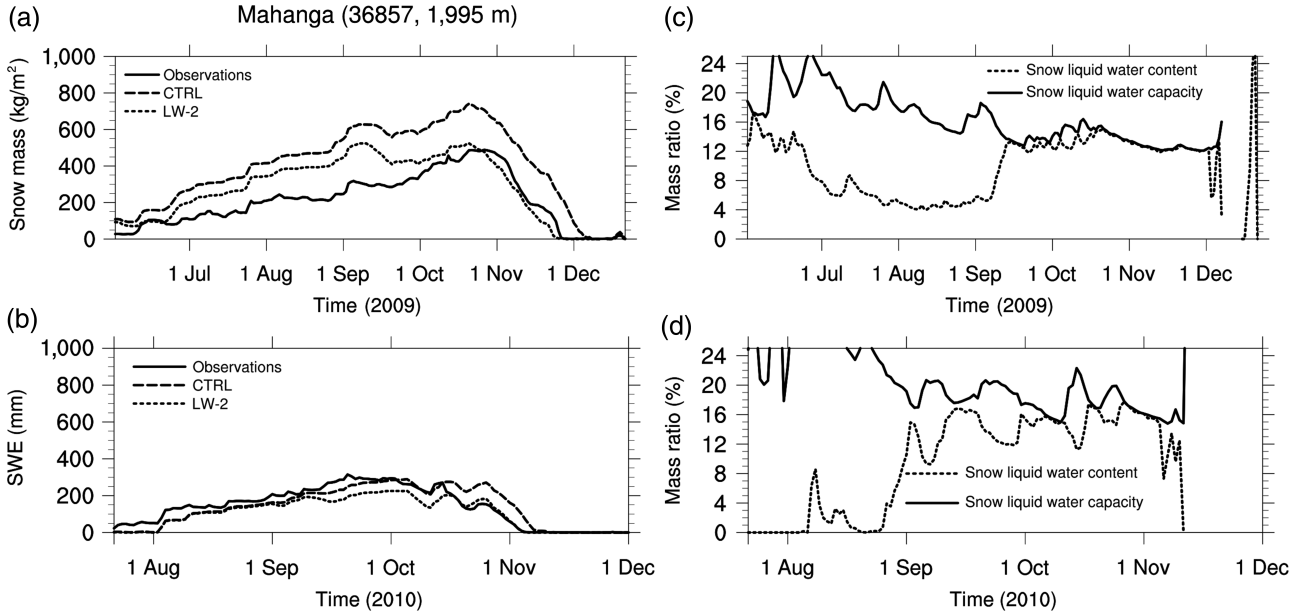

FIGURE 5 As for Figure 4, but for Mahanga in 2009 and 2010. The downward long wave radiation (LW-2) is the sensitivity test of the LW, as described in Section 5.1

TABLE 1 Descriptions of sensitivity tests for different compactive factor (η), critical air temperature for snow (T_c), downward long wave radiation at the surface (LW) and the snow albedo schemes (Essery *et al.*, 2001)

Tests	η (Pa s)	T_c (K)	Snow albedo scheme	Long wave radiation (LW)
CTRL	2×10^7	274.0	Spectral	No bias correction
LW-1	2×10^7	274.0	Spectral	**Bias correction of 6.1 W/m^2 at Mueller Hut**
LW-2	2×10^7	274.0	Spectral	**Bias correction of 6.1 W/m^2 at Mahanga**
TEST1	2×10^7	**273.8**	Spectral	No bias correction
TEST2	2×10^7	**273.5**	Spectral	No bias correction
TEST3	$\mathbf{1 \times 10^7}$	274.0	Spectral	No bias correction
ALB-1	2×10^7	274.0	**All-band**	No bias correction

Notes: Changes in parameter values for setting the sensitivity tests are shown in bold.
For definitions of tests, see the text.

Overall, significantly higher simulated SWE (about 20–50% of the observed SWE) than that observed is a dominant feature at the two sites. This may have resulted from more precipitation falling as snow in the JULES, which could be caused by errors in albedo or use of a higher T_c than it should be. In addition, a higher simulated SWE could also be due to less snowmelt. Raleigh *et al.* (2016) investigated which forcing would have most impact on simulations of snowpack mass and energy states. They found that incoming LW, which is measured least frequently, caused the greatest divergences in model behaviour. In the present study, the LW simulated by the NZLAM was used because it was not measured at the two sites. The bias and errors in the simulated LW may be a factor in the simulated SWE errors described above. The sensitivity of the snow simulation to errors in the simulated LW, albedo and T_c is investigated in Section 5.

4.2 | Snow density

In the multilayer snow scheme, snow density is a prognostic variable. Given snow mass, the snow depth is derived from snow density. Thus, the simulated snow density was verified in the present study rather than snow depth. The observed snow density was calculated by using hourly SWE and snow depth observations.

A common feature at the two sites for most of the time is that the simulated snow density was lower (≤ 200 kg/m^3) than observations (Figure 6), especially during snowmelt periods: from mid-October 2010 (Figure 6a) and from the end of

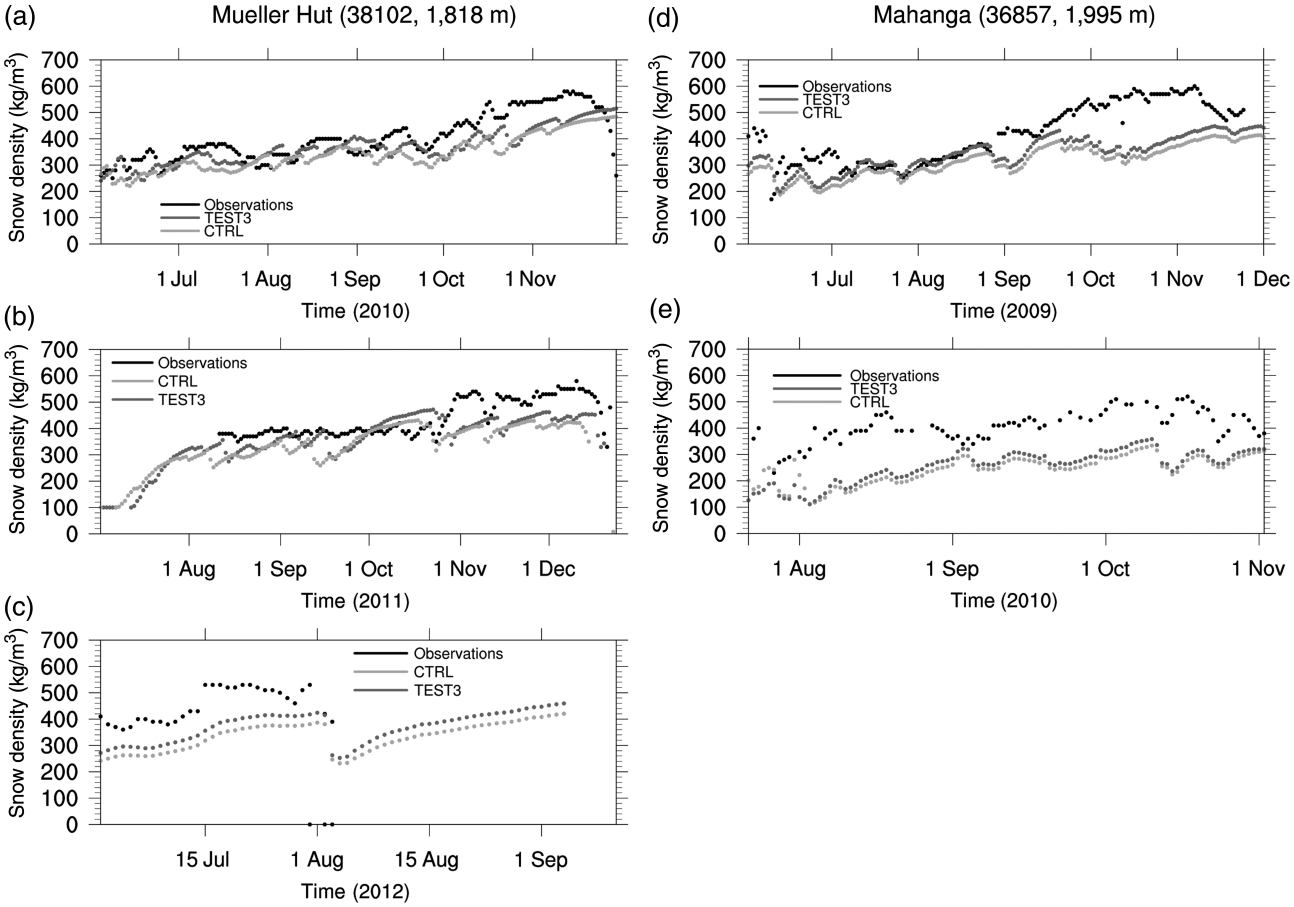

FIGURE 6 Simulated and observed snow densities at Mueller Hut in (a) 2010, (b) 2011 and (c) 2012, and at Mahanga in (d) 2009 and (e) 2010. The density of very shallow snow (< 10 cm) had large variations and is not shown. See Table 1 and Section 5.4 for TEST3

October 2011 (Figure 6b) at Mueller Hut, and from the end of September 2009 at Mahanga (Figure 6d). Snow density is proportional to snow mass (Equation 2). As shown above, the simulated SWE did not have a dominant negative bias, and in some years the simulated SWE was even higher than the observations. Thus, the negative bias in simulated snow density was not due to errors in the simulated SWE. Section 5 investigates whether the parameter settings in the snow density parameterization scheme are responsible for the bias in simulated snow density.

Generally, periods with lower snow (about ≤ 0.5 m) in 2012 at Mueller Hut (Figure 6c) and 2010 at Mahanga (Figure 6e) have a larger negative bias in density than periods with deep snow. Part of the larger bias is very likely due to errors in observations because for the same error magnitude in snow depth and mass, shallower snow tends to have larger errors in the calculated snow density than a deeper snow.

5 | SENSITIVITY TESTS

A set of tests of sensitivity to various parameter settings was conducted. The list is shown in Table 1. The subsections within this section describe the different sensitivities found.

5.1 | Long wave radiation (LW)

Observations of downward LW at the surface are quite rare in New Zealand. Fortunately, however, from 7 June to 28 July 2014, during the DEEPWAVE (Fritts *et al.*, 2015), LW observations were made at Hokitika on the west side of the central South Island of New Zealand. These LW data have helped to determine the possible errors in the LW simulated by the NZLAM. During this period, the simulated downward LW had a bias (simulation–observations) of 6.1 W/m^2 and a mean absolute error of 12.3 W/m^2.

Assuming that the simulated LW used in the CTRL at Mueller Hut and Mahanga also had a similar bias to that at Hokitika, two tests were run in which the downward LW at Mueller Hut (LW-1) and Mahanga (LW-2) (Table 1) was increased by 6.1 W/m^2.

At Mueller Hut (Figure 4), relatively large differences in the simulated SWE (snow ice plus snow liquid water) were found between the CTRL and the LW-1 throughout 2010 (Figure 4a) and during the snowmelt period after October 2011 (Figure 4b). At Mahanga, large differences in the simulated SWE between the CTRL and the LW-2 were found for 2009 (Figure 5a). Large differences were also found after

mid-September 2010 (Figure 5b). These experiments indicate that errors in the simulated LW for the CTRL can have large effects on the simulated amount of snow. At Mueller Hut, this effect increased the errors in simulated snow throughout 2010 (Figure 4a), but decreased the errors during snowmelt in 2011 (Figure 4b), and had little effect in 2012 (Figure 4c). Overall, the bias in the simulated LW (CTRL) increased errors in the simulated SWE at Mueller Hut. At Mahanga, the bias in the simulated LW (CTRL) largely increased the errors in the simulated snow (Figure 5a) throughout 2009. In 2010 (Figure 5b), the bias in the LW decreased the errors before mid-October and increased the errors after that period. Thus, bias and errors in the simulated LW are very likely major factors contributing to the errors in the simulated SWE.

The bias in the LW did not affect the simulation at Mueller Hut until early September 2011 and had no effect at all in the winter of 2012, in contrast to 2010 (Figure 3a–c). At Mahanga (Figure 4a,b), the bias in the LW did not affect the snow simulation until early September 2010, in contrast to 2009. A check of the snow liquid water content and snow liquid water capacity (SLWC), that is, the maximum liquid water content in snow without runoff (Figures 4d–f and 5c, d), for the CTRL produced similar findings. Large differences between the CTRL and the LW-1 or LW-2 in the simulated SWE were found only when a significant amount of snow liquid water (with respect to the SLWC) occurred in snow. This included the whole snow season of 2010 and during the spring from early September 2011 at Mueller Hut (Figure 4), and the whole snow season in 2009 and during the spring from 1 September 2010 at Mahanga (Figure 5). For time periods with small differences in the simulated SWE, little or no liquid water was found in snow.

For the periods with little or no liquid water in snow, the snow temperature was well below 0°C. When the LW was decreased, no liquid water was available to freeze to form ice. For a small increase in the LW (LW-1 and LW-2), there was almost no snowmelt and the SWE remained the same. As a result, the simulated SWE in the LW-1 and LW-2 was almost the same as in the CTRL for the periods with little or no liquid water in snow.

For periods with significant liquid water (about half the SLWC or more) in snow, especially during the spring, the snow temperature was very close to 0°C. This allowed a small increase in the LW to melt some ice into liquid water for the LW-1 and LW-2. Part of the liquid water was stored in the snow and part of it water was lost after the SLWC was reached during snow accumulation, or almost all the liquid water melt from snow was lost during a snowmelt period with the snow liquid water content reaching the SLWC. The snow liquid water was lost either as runoff or by absorption into the soil (data not shown). This analysis showed that small errors in the LW significantly affected the SWE simulations only when a significant amount of liquid water was found in snow during spring and relatively warm winters.

5.2 | Snow albedos

The bias and errors in the LW impact the simulations of the SWE through their impact on the surface energy budget calculations (Equation 1). Small bias and errors in the LW are equivalent to small errors in albedo (or the SW, emissivity, sensible and latent heat fluxes, or heat flux into and out of the snow surface). For the LW-1 and LW-2, the bias (about 6 W/m^2) in the LW accounted for about 3% of the annual mean downward LW at Mueller Hut and Mahanga. This magnitude of the bias in the LW is equivalent to about 5% of the annual mean downward SW at the two sites, or equivalent to the contribution of the errors of about 0.05 in the snow surface albedo α (Equation 1). To verify this, snow simulations were also conducted at both sites by decreasing the prognostic snow albedo for the SW by 0.05. The simulated SWE was almost the same as the LW-1 at Mueller Hut and the LW-2 at Mahanga (data not shown). Previous studies (Roesch, 2006; Randall *et al*., 2007; Essery *et al*., 2013; Chen *et al*., 2014) indicated that using the correct albedo over the snow region is an important area for model development because of large errors and large variations among snow models when simulating snow albedo.

To investigate the effect of albedo on snow simulation, another sensitivity test called ALB-1 was conducted (the albedo test) (Table 1). The JULES has two different snow albedo schemes: all-band albedo and spectral albedo (Essery *et al*., 2001). For the former, the snow albedos are calculated based on the prescribed snow albedos for soil and the five vegetation types in the JULES, and the snow ageing and snow mass. For the latter, the snow albedos are calculated using a simplification of the Marshall (1989) parameterization of the Wiscombe and Warren (1980) spectral snow albedo model. Fresh snow albedos are 0.98 for visible and 0.7 for near infrared. The ageing of snow is characterized by the prognostic grain size of snow.

At Mueller Hut and Mahanga (Figures 7 and 8), the albedos calculated by the ALB-1 had larger temporal variations than those from the spectral albedo scheme (CTRL) during the periods with snow cover, and were overall lower (≤ 0.2). Lower albedos for the ALB-1 let snow absorb more solar energy than the CTRL. This led to more snowmelt, less snow accumulation and earlier termination of snow cover for the ALB-1 than the CTRL. Quite large differences in albedos (≤ 0.6) between the CTRL and the ALB-1 were found during the end of the snow season when snow cover was found for the CTRL but not for the ALB-1.

At Mueller Hut in 2010 (Figure 7a), the ALB-1 test had smaller errors in the simulated SWE than the CTRL during the snow accumulation periods before mid-October. During the snowmelt periods, the ALB-1 test had negative bias, while the CTRL had almost the same magnitude of positive bias. In 2011 (Figure 7b), the CTRL and ALB-1 were almost the same before October. After that, the ALB-1 had much less snow accumulation than the CTRL. In 2012 (Figure 7c), the CTRL and ALB-1 were almost the same. At Mahanga in 2010 (Figure 8a), more snowmelt for the ALB-1 test led to smaller errors than for the CTRL before October. After that, the ALB-1 had a negative bias while the CTRL had a positive bias. In 2010 (Figure 8b), large differences between the CTRL and the ALB-1 occurred in snow simulations after September. At the two sites, the differences in albedos between the CTRL and the ALB-1 led to large differences in the simulated SWE, mainly during the snowmelt season (spring) and relatively warm winters (2010 at Mueller Hut and 2009 in Mahanga). These features were almost the same as those found for the LW-1 and LW-2, except that the ALB-1 had much lower snow accumulation due to much lower snow albedos. This experiment indicated that errors in snow albedos had a large effect on snow simulation in New Zealand, and the influence mainly occurred during the snowmelt season and in winters when significant snow liquid water was present in snow.

5.3 | Sensitivity to air temperature for snow occurrence

Air temperature for snow occurrence (T_c) controls what precipitation is snowfall in snow models. Slight differences in T_c can be found among snow models. Jennings *et al.* (2018) found an average T_c of 1.0°C (range = 0.4–2.4°C) for the Northern Hemisphere. Continental climates generally exhibit the highest T_c and maritime the lowest T_c. In the CTRL, T_c was set to 274.0 K, close to the average. This may be slightly higher than it should be for the maritime climate of New Zealand. In the present study, sensitivity tests for different values of T_c were conducted. TEST1 ($T_c = 273.8$ K) and TEST2 ($T_c = 273.5$ K) (Table 1) have slightly lower values of T_c than the CTRL (274.0 K). This decreased the snowfall with less SWE (smaller errors) at Mueller Hut, as shown in 2010 for the TEST1 and TEST2 (Figure 9a). However, there was almost no difference in the simulated SWE between the CTRL and the TEST1 or TEST2 in 2011 and 2012

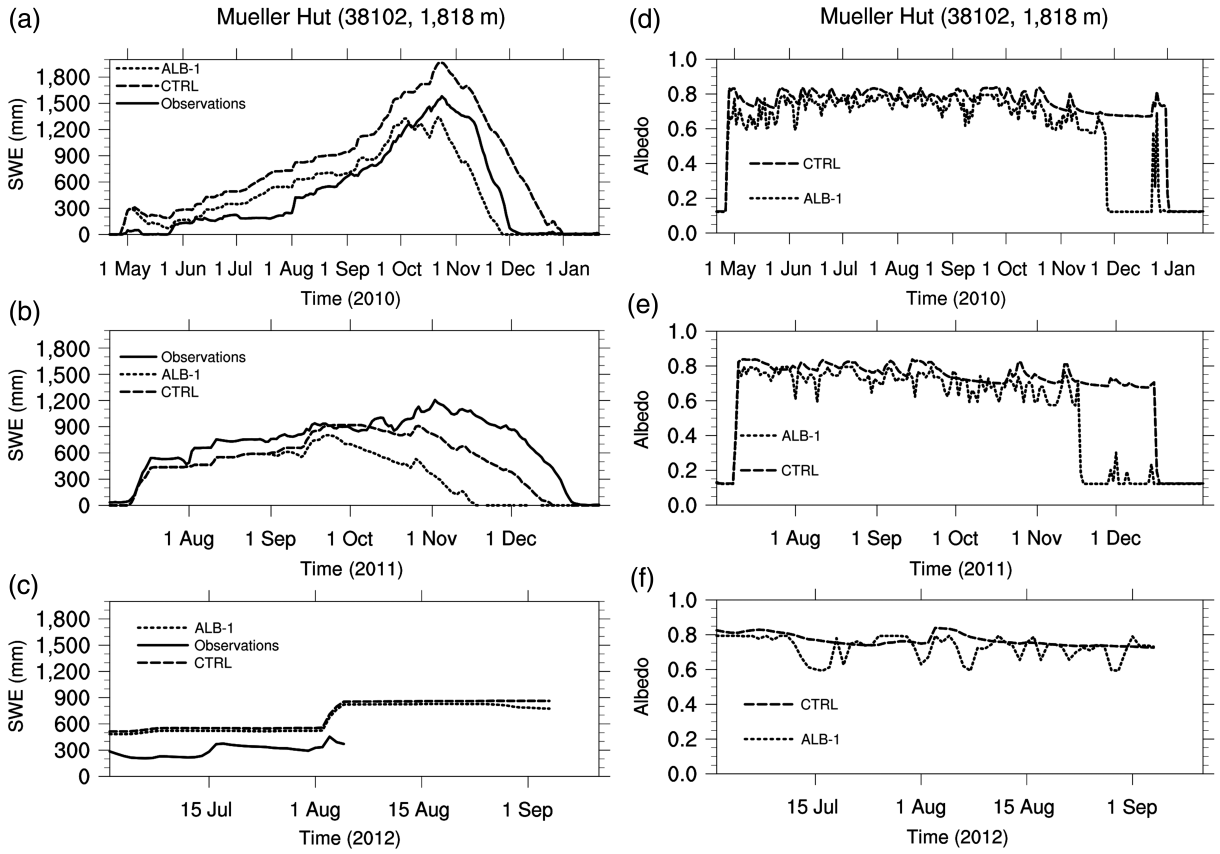

FIGURE 7 Simulated and observed snow water equivalents (SWEs) in (a) 2010, (b) 2011 and (c) 2012, and simulated albedos in (d) 2010, (e) 2011 and (f) 2012 by the control simulation with default settings in the Joint UK Land Environment Simulator (JULES) (CTRL) and the ALB-1 (the albedo test) at Mueller Hut, respectively

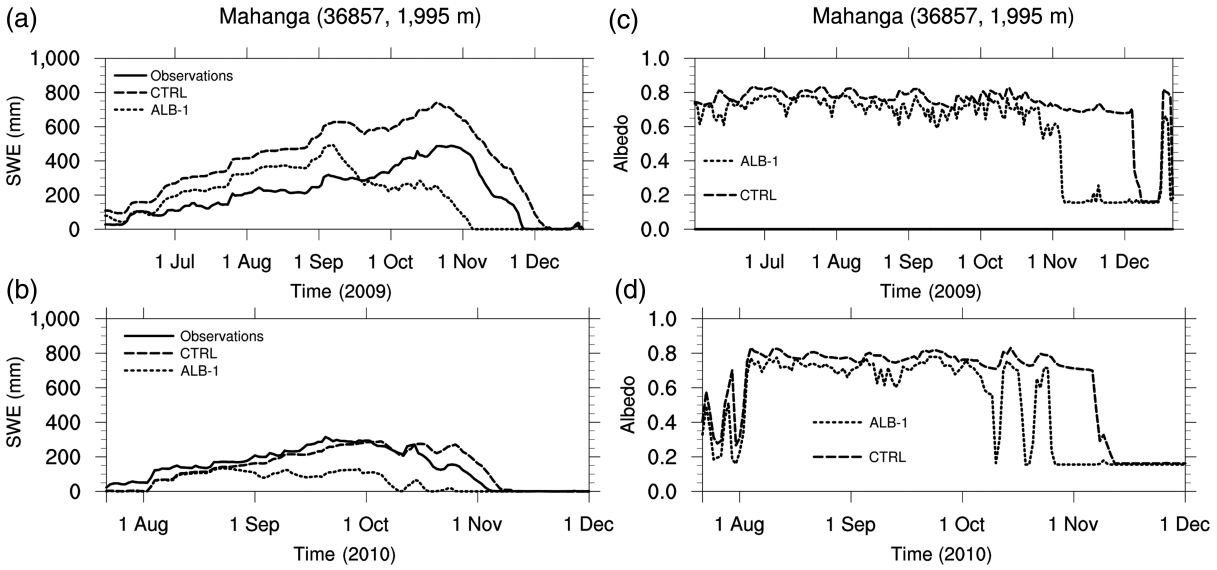

FIGURE 8 As for Figure 7, but for Station Mahanga in 2009 and 2010

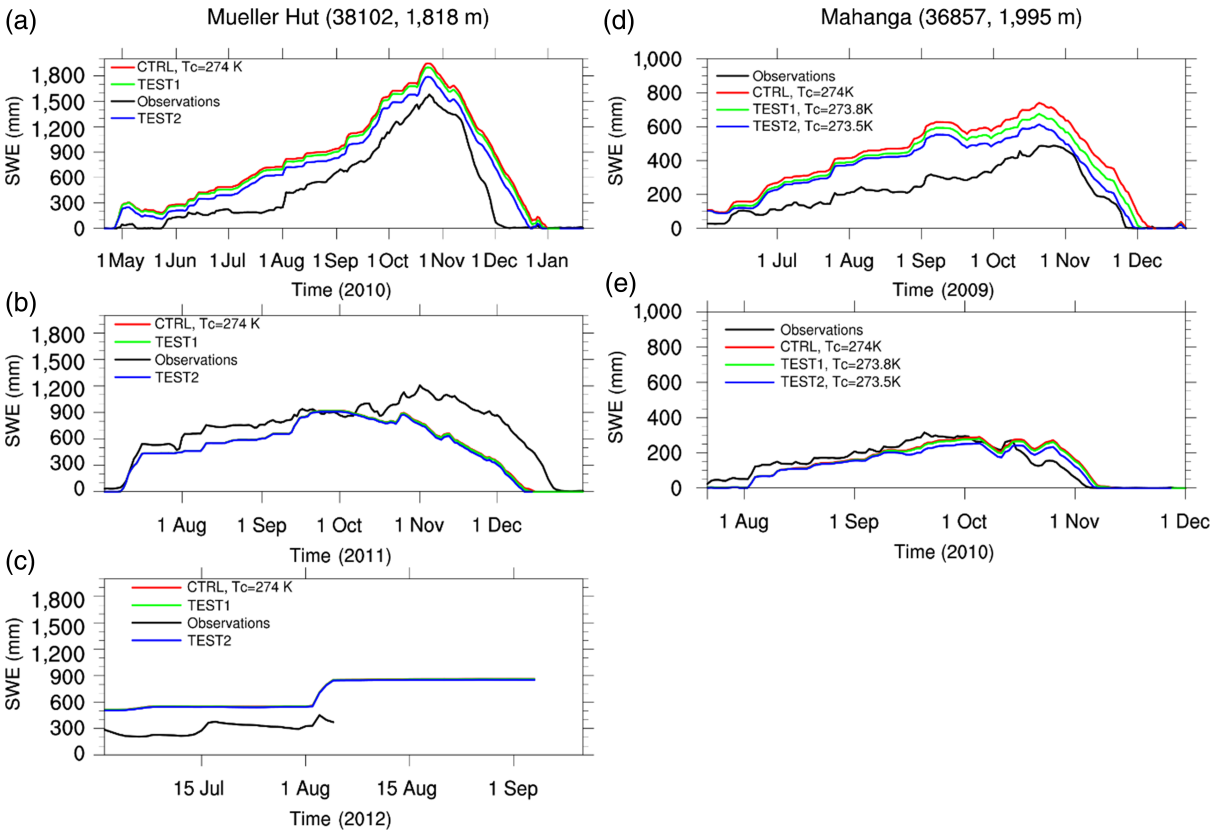

FIGURE 9 Observed and simulated snow water equivalents (SWEs) by the CTRL, TEST1 and TEST2 at Mueller Hut in (a) 2010, (b) 2011 and (c) 2012, and at Mahanga in (d) 2009 and (e) 2010, respectively. See Table 1 for descriptions of TEST1 and TEST2

	CTRL	TEST1	TEST2	LW-1	LW-2	ALB-1
Mueller Hut	93 (**189**)	83 (**180**)	57 (**159**)	66 (**176**)		−38 (**172**)
Mahanga	40 (**52**)	34 (**46**)	26 (**40**)		15 (**35**)	−10 (**40**)

TABLE 2 Bias (simulation–observations) and mean absolute errors (shown in bold) of the simulated snow water equivalent (SWE) (mm) at Mueller Hutt and Mahanga for the CTRL and the sensitivity tests

Note: For definitions of tests, see the text.

(Figure 9b,c). In 2010, much more precipitation occurred between 273.5 and 274.0 K at Mueller Hut than in 2011 and 2012. Similar results at Mueller Hut in 2010 were also found at Mahanga in 2009 and 2010 (Figure 9d,e). A decrease in T_c from 274.0 to 273.5 K decreased the errors in the simulated mass by up to one-third at Mueller Hut in 2010 and by up to half at Mahanga in spring 2009. During the snowmelt season in 2010 at Mahanga, a decrease in T_c also decreased the errors. As described above, the two years at the two stations were relatively warm with significant snow liquid water present compared with the SLWC. These results indicate that for relatively warm years with significant precipitation, the T_c can be a major factor affecting snow simulation. A T_c of 274 K is higher than it should be over the mountains of the South Island in a maritime climate. A more reasonable value would be 273.5 K or slightly smaller. This is consistent with the results from observational study by Jennings *et al*. (2018) for the Northern Hemisphere.

The simulated snow density was almost the same at Mueller Hut and Mahanga for the CTRL, TEST1 and TEST2 in all three years (data not shown), indicating that T_c is not a major factor for the bias in simulated snow density in the CTRL for the years studied.

5.4 | Parameters in snow density estimation

For the snow density forecast Equation 2, a smaller η can reduce the negative bias in simulated snow density. The effect of k_s is determined by the balance of $(\frac{k_s}{T_m} - \frac{k_s}{T_k})$. Since T_m and T_k are very close, the simulated snow density is not very sensitive to the variation of k_s. In this section, a sensitivity test (TEST3) (Table 1) of snow density to η was conducted.

In the CTRL experiment, the compactive factor η was set as 20×10^6 in the JULES. This η is above the recommended value range ($5 \times 10^6 - 14 \times 10^6$ Pa s). In this test, the η was changed from 2×10^7 to 1×10^7 Pa s. Figure 6 shows the simulated snow density with $\eta = 1 \times 10^7$ (TEST3) and snow density observations. The observed snow density could be up to about 600 kg/m^3 at the two sites. For snow depth > 100 mm, the biases of snow density for TEST3 were −33.7, −44.8 and −100.6 kg/m^3 at Mueller Hut for 2010, 2011 and 2012, respectively. In contrast, for the CTRL they were −59.3, −70.1 and −135.8 kg/m^3. At Mahanga for TEST3, they were −74.5 and −140.2 kg/m^3 for 2009 and 2010, respectively. However, for the CTRL they were −104.7 and −160.1 kg/m^3, respectively. The bias of the TEST3 was significantly lower than that of the CTRL, indicating that an inappropriate value of η is a key factor that could lead to the bias in simulated snow density.

6 | CONCLUSIONS

Over the South Island of New Zealand, snow frequently occurs during winter in a maritime climate. The seasonal snow accumulation in early spring could be 3,000–4,000 mm deep at some locations, which significantly influences the New Zealand economy by affecting hydroelectricity generation, agricultural irrigation and recreational sectors dependent on snow. Owing to a lack of snow observations, snow simulations and validation of the snow models over New Zealand have been limited. Most of the verification of snow simulations have been more qualitive than quantitive. Key factors affecting snow simulations in New Zealand were not well known.

In the present study, the SWE and snow density simulated by the multilayer snow scheme of the JULES were verified by using observations at two sites in high mountainous areas of the South Island. To the authors' knowledge, this is the first time the performance of the multilayer snow scheme of the JULES has been tested over islands with a humid and relatively warm maritime climate:

- The model simulated well the periods of snow accumulation and the time of occurrence of maximum snow accumulation. However, for relatively warm winters with heavy snow (2010 at Mueller Hut and 2009 at Mahanga), the simulated snowmelt in spring lasted longer than that observed. Large errors (≤ 300 mm SWE, about 20–50% of the observed SWE) were found during part of winter and the snowmelt period.
- Sensitivity tests showed that small errors in the downward LW at the surface and in snow albedos could lead to relatively large errors in the simulated SWE (100–200 mm) during snowmelt in spring and relatively warm periods in winter when the liquid water in snow was about half the SLWC or more, indicating that errors in the simulated

LW and snow albedos are potentially two important factors leading to the large errors in the simulated SWE.

- Air temperature for snow (T_c) is a required parameter for the JULES standalone version. In the present study, T_c was found to be another potentially important factor affecting the simulated SWE for relatively warm years with significant precipitation occurring around the T_c. For the maritime climate of New Zealand, $T_c = 274$ K is very likely higher than it should be. Modelling suggests a better value would be 273.5 K or slightly smaller.
- The observed snow density at the two sites ranged from 50 to 200 kg/m^3 for fresh snow and about 600 kg/m^3 for deep snow. The simulated snow density had a negative bias, especially during snowmelt. The sensitivity test conducted here showed that using a higher value of the compactive factor η in the snow density prognostic equation had a major influence. Based on the quality of the current observation data at the two sites, the best η value should be 1×10^7 Pa s or slightly lower.

7 | DISCUSSION

The snow simulation showed that for snow liquid water, about half or more of the SLWC was present not only in spring but also in some winters. This implied a relatively warm and wet snowpack over New Zealand under a maritime climate. This is consistent with previous observation studies (Fitzharris *et al*., 1999). The relatively warm and humid maritime climate of New Zealand made the snow simulation for the country sensitive to the downward long wave radiation (LW) and albedo not only in spring but also in some winters. This may be a significant difference in snow simulation between New Zealand and the continents. The relatively warm and humid maritime climate of New Zealand may make its snow simulation more sensitive to the LW and snow albedos than in continental areas.

At the two stations, the spectral albedo scheme (CTRL) (Table 1) simulation produced more snow water equivalent (SWE) than observations, while the ALB-1 (the albedo test) (Table 1) simulation produced overall less SWE during the snowmelt season than observations and less SWE than the CTRL run during most of the winter. The snow albedos calculated by the spectral albedo scheme (CTRL) were overall higher (0.05–0.2) than those calculated by the all-band albedo scheme (ALB-1). These results seem to suggest that the albedos calculated by the ALB-1 were lower than they should be and those from the spectral albedo scheme were higher. This is supported by the results from the snow simulation using the Joint UK Land Environment Simulator (JULES) multilayer snow scheme in Norway by Vikhamar-Schuler *et al*. (2012), which show the fact that decreasing the snow albedo calculated from the spectral scheme leads to better results. However, verification of snow albedos at the two sites was not performed because there were no albedo observations, but these will be done in future when snow albedo observations become available over New Zealand.

Surrounded by the relatively warm seas of the southwest Pacific, New Zealand has a generally humid maritime climate. However, the two major islands, South and North, span about 12° latitude from about 35 to about 47° S and consist of mountains with different elevations. This suggests that a uniform T_c may not be suitable for all New Zealand. In addition, using T_c alone may not be the best way to determine precipitation phase. Including other meteorological fields, for example, relative humidity, dew point temperature, wet-bulb temperature or a combination of them (Feiccabrino *et al*., 2015) may be a better way. When the JULES is coupled with the Met Office's Unified Model (UM), T_c is not a control parameter. The precipitation phase is determined by the simulated air temperature and moisture profiles, and the cloud and precipitation schemes of the atmosphere model. Because of errors in the model initial conditions, model physics schemes and in lower boundary conditions, this phase determination may have large errors. For snow simulation in New Zealand, more research is needed to know which way is better for determining the precipitation phase.

In addition to the effect of the compactive factor η, there could be other reasons for the bias of the simulated snow density. Equation 2 is based on experiments performed by Kojima (1966) on snow cover density for snow temperatures in the range of 268–273 K and for fresh snow densities of 50–70 kg/m^3. In the present study, the fresh snow density was taken as 100 kg/m^3. The difference in the snow characteristics may be a reason for the snow density bias. In Equation 2, another term was neglected: the metamorphic processes (Boone and Etchevers, 2001). Wet snow metamorphic processes are likely to be relevant in the New Zealand alpine context and would be something to focus on in future work.

In the present study, snow simulations were conducted for only two to three years at two stations. This is a small number of sites and years. However, these snow and meteorological observations are the only data available so far in New Zealand that can be used to run the JULES. Even though quite large seasonal and annual variations in the SWE were found at the two sites, the results from the sensitivity tests at the two sites for the available years are almost the same. This can be further found from the biases (simulation–observations) and mean absolute errors of the SWE for all the sensitivity tests shown in Table 2. At the two sites, a slightly decreased T_c from 274 K (TEST1 and TEST2) significantly decreased the positive biases and errors of the simulated SWE. Increasing the downward LW

(LW-1 and LW-2) also significantly decreased the biases and errors. Using the all-band scheme to calculate the snow albedo, the errors of the simulated SWE at the two sites were significantly decreased, but with a negative bias compared with the CTRL. These analyses support the robustness of the conclusions.

ACKNOWLEDGEMENTS

This research was carried out under research collaboration number SC0128 with the UK Met Office and funded by the National Institute of Water & Atmospheric Research (NIWA) under its Hazards Research Programme (2015/16 and 2016/17 SCI). The authors thank Mr Andrew Willsman (andrew.willsman@niwa.co.nz) of NIWA for providing the quality-checked snow data. All the data used in the present study can be accessed at the climate data archive of NIWA (https://cliflo.niwa.co.nz). The authors also thank the members of the DEEPWAVE project for the use of the long wave observations in the present study.

ORCID

Yang Yang https://orcid.org/0000-0002-8732-2349

ENDNOTE

[1] For the multilayer snow scheme of JULES, it is suggested that the total minimum thickness of snow layers (m) are four or more. Seven snow layers was set in the present study, but the results are almost the same as for six or five snow layers.

REFERENCES

Albert, M.R. (2002) Effects of snow and firn ventilation on sublimation rates. *Annals of Glaciology*, 35, 510–514.

Arons, E.M. and Colbeck, S.C. (1995) Geometry of heat and mass transfer in dry snow: a review of theory and experiment. *Reviews of Geophysics*, 33, 463–493.

Best, M.J., Pryor, M., Clark, D.B., Rooney, G.G., Essery, R.L.H., Ménard, C.B., Edwards, J.M., Hendry, M.A., Porson, A., Gedney, N., Mercado, L.M., Sitch, S., Blyth, E., Boucher, O., Cox, P.M., Grimmond, C.S.B. and Harding, R.J. (2011) The Joint UK Land Environment Simulator (JULES), model description – Part 1: energy and water fluxes. *Geoscientific Model Development*, 4, 677–699. https://doi.org/10.5194/gmd-4-677-2011.

Boone, A. and Etchevers, P. (2001) An intercomparison of three snow schemes of varying complexity coupled to the same land surface model: local-scale evaluation at an alpine site. *Journal of Hydrometeorology*, 2, 374–394.

Chen, F., Barlage, M., Tewari, M., Rasmussen, R., Jin, J., Lettenmaier, D., Livneh, B., Lin, C., Miguez-Macho, G., Niu, G. Y., Wen, L. and Yang, Z.L. (2014) Modeling seasonal snowpack evolution in the complex terrain and forested Colorado Headwaters region: a model intercomparison study. *Journal of Geophysical Research – Atmospheres*, 119, 13795–13819. https://doi.org/10.1002/2014JD022167.

Clark, M., Hendrikx, J., Slater, A., Kavetski, D., Anderson, B., Cullen, N., Kerr, T., Örn Hreinsson, E. and Woods, R. (2011) Representing spatial variability of snow water equivalent in hydrologic and land-surface models: a review. *Water Resources Research*, 47, W07539. https://doi.org/10.1029/2011WR010745.

Cox, P.M., Betts, R., Bunton, C., Essery, R., Rowntree, P. and Smith, J. (1999) The impact of new land surface physics on the GCM simulation of climate and climate sensitivity. *Climate Dynamics*, 15, 183–203.

Dirmeyer, P.A., Gao, X., Zhao, M., Guo, Z., Oki, T. and Hanasaki, N. (2006) GSWP-2: multimodal analysis and implications for our perception of the land surface. *Bulletin of the American Meteorological Society*, 87, 1381–1397.

Essery, R., Best, M. and Cox, P. (2001) *MOSES2.2 Technical Document*. Hadley Centre technical note 30. Met Office.

Essery, R., Rutter, N., Pomeroy, J., Baxter, R., Stahli, M., Gustafsson, D., Barr, A., Bartlett, P. and Elder, K. (2009) SNPWMIP2, an evaluation of forest snow process simulations. *Bulletin of the American Meteorological Society*, 90, 1120–1135.

Essery, R., Morin, S., Lejeune, T. and Menard, C. (2013) A comparison of 1701 snow models using observations from an alpine site. *Advances in Water Resources*, 55, 131–148.

Etchevers, P., Martin, E., Brown, R., Fierz, C., Lejeune, Y., Bazile, E., Boone, A., Dai, Y., Essery, R., Fernandez, A., Gusev, Y., Jordan, R., Koren, V., Kowalczyk, E., Nasonova, N., Pyles, R., Schlosser, A., Shmakin, A., Smirnova, T., Strasser, U., Verseghy, D., Yamazaki, T., & Yang, Z. (2004). Validation of the energy budget of an alpine snowpack simulated by several snow models (Snow MIP project). *Annals of Glaciology*, 38, 150–158.

Feiccabrino, J., Graff, W., Lundberg, A., Sandström, N. and Gustafsson, D. (2015) Meteorological knowledge useful for the improvement of snow rain separation in surface based models. *Hydrology*, 2, 266–288. https://doi.org/10.3390/hydrology2040266.

Feng, X., Sahoo, A., Arsenault, K., Houser, P., Luo, Y. and Troy, T. (2008) The impact of snow model complexity at three CLPX sites. *Journal of Hydrometeorology*, 9, 1464–1481.

Fitzharris, B. and Garr, C. (1995) Simulation of past variability in seasonal snow in the Southern Alps, New Zealand. *Annals of Glaciology*, 21, 377–382.

Fitzharris, B., Lawson, W. and Owens, I. (1999) Research on glaciers and snow in New Zealand. *Progress in Physical Geography*, 23(4), 469–500.

Fritts, D., Smith, R.B., Taylor, M.J., Doyle, J.D., Eckermann, S.D., Dörnbrack, A., Rapp, M., Williams, B.P., Pautet, P.D., Bossert, K., Criddle, N.R., Reynolds, C.A., Reinecke, P.A., Uddstrom, M., Revell, M.J., Turner, R., Kaifler, B., Wagner, J.S., Mixa, T., Kruse, C.G., Nugent, A., Watson, C., Gisinger, S., Smith, S., Lieberman, R., Laughman, B., Moore, J., Brown, W., Haggerty, J., Rockwell, A., Stossmeister, G., Williams, S., Hernandez, G., Murphy, D., Klekociuk, A., Reid, I. and Ma, J. (2015) The Deep Propagating Gravity Wave Experiment (DEEPWAVE): an airborne and ground-based exploration of gravity wave propagation and effects from their sources throughout the lower and middle atmosphere. *Bulletin of the American Meteorological Society*, 97, 425–453. https://doi.org/10.1175/BAMS-D-14-00269.1.

Gunther, D., Marke, T., Essery, R. and Strasser, U. (2019) Uncertainties in snowpack simulations--assessing the impact of model

structure, parameter choice, and forcing data error on point-scale energy balance snow model performance. *Water Resources Research*, 55, 2779–2800.

Gustafsson, D., Stähli, M. and Jansson, P.E. (2001) The surface energy balance of a snow cover: comparing measurements to two different simulation models. *Theoretical and Applied Climatology*, 70, 81–96.

Jennings, K., Winchell, S.T., Livneh, B. and Molotch, N. (2018) Spatial variation of the rain–snow temperature threshold across the Northern Hemisphere. *Nature*, 9, 1148.

Kojima, K. (1966) Densification of seasonal snow cover. In Proceedings, International Conference on Low Temperature Science, 14–19 August 1966, Sapporo, Japan, pp. 929–952

Lemke, P., Ren, J., Alley, R.B., Allison, I., Carrasco, J., Flato, G., Fujii, Y., Kaser, G., Mote, P., Thomas, R.H. and Zhang, T. (2007) Observations: changes in snow, ice and frozen ground. In: Solomon, S., Qin, D., Manning, M., Chen, Z., Marquis, M., Averyt, K.B., Tignor, M. and Miller, H.L. (Eds.) *Climate Change 2007: The Physical Science Basis, in Contribution of Working Group I to the Fourth Assessment Report of the Intergovernmental Panel on Climate Change*. New York, NY: Cambridge University Press, pp. 339–378.

Lynch-Stieglitz, M. (1994) The development and validation of a simple snow model for the GISS GCM. *Journal of Climate*, 7, 1842–1855.

Marshall, S.E. (1989) *A physical parametrization od snow albedo for use in climate models*. NCAR Cooperative Thesis 123, NCAR, Boulder, CO.

McKerchar, A., Pearson, C. and Fitzharris, B. (1998) Dependency of summer lake inflows and precipitation on spring SOI. *Journal of Hydrology*, 205, 66–80.

Owens, I. and Fitzharris, B. (2004) Seasonal snow and water. In: Harding, J., Mosley, P., Pearson, C. and Sorrell, B. (Eds.) *Freshwaters of New Zealand*, Chap. 6. Christchurch: Caxton Press.

Parajka, J., Dadson, S., Lafon, T. and Essery, R. (2010) Evaluation of snow cover and depth simulated by a land surface model using detailed regional snow observations from Austria. *Journal of Geophysical Research*, 115, D24117. https://doi.org/10.1029/2010JD014086.

Pitman, A.J., Yang, Z.L., Cogley, J.G. and Henderson-Sellers, A. (1991) *Description of Bare Essentials of Surface Transfer for the Bureau of Meteorological Research Centre AGCM*, p. 1991.

Raleigh, M.S., Livneh, B., Lapo, K. and Lundquist, J.D. (2016) How does availability of meteorological forcing data impact physically based snowpack simulations? *Journal of Hydrometeorology*, 17, 99–120.

Randall, D.A., Wood, R.A., Bony, S., Colman, R., Fichefet, T., Fyfe, J., Kattsov, V., Pitman, A., Shukla, J., Srinivasan, J., Stouffer, R.J., Sumi, A. and Taylor, K.E. (2007) Climate models and their evaluation. In: Solomon, S., Qin, D., Manning, M., Chen, Z., Marquis, M., Averyt, K.B., Tignor, M. and Miller, H.L. (Eds.) *Climate Change 2007: The Physical Science Basis. Contribution of Working Group I to the Fourth Assessment Report of the Intergovernmental Panel on Climate Change*. Cambridge and New York, NY: Cambridge University Press, pp. 589–662.

Roesch, A. (2006) Evaluation of surface albedo and snow cover in AR4 coupled climate models. *Journal of Geophysical Research*, 111, D15111. https://doi.org/10.1029/2005JD006473.

Rutter, N., Essery, R., Pomeroy, J., Altimir, N., Andreadis, K., Baker, I., Barr, A., Bartlett, P., Boone, A., Deng, H., Douville, H., Dutra, E., Elder, K., Ellis, C., Feng, X., Gelfan, A., Goodbody, A., Gusev, Y., Gustafsson, D., Hellström, R., Hirabayashi, Y., Hirota, T., Jonas, T., Koren, V., Kuragina, A., Lettenmaier, D., Li, W.-P., Luce, C., Martin, E., Nasonova, O., Pumpanen, J., Pyles, R.D., Samuelsson, P., Sandells, M., Schädler, G., Shmakin, A., Smirnova, T.G., Stähli, M., Stöckli, R., Strasser, U., Su, H., Suzuki, K., Takata, K., Tanaka, K., Thompson, E., Vesala, T., Viterbo, P., Wiltshire, A., Xia, K., Xue, Y. and Yamazaki, T. (2009) Evaluation of forest snow processes models (SnowMIP2). *Journal of Geophysical Research*, 114, D06111.

Slater, A.G., Schlosser, C.A., Desborough, C.E., Pitman, A.J., Henderson-Sellers, A., Robock, A., Vinnikov, K.Y., Entin, J., Mitchell, K., Chen, F., Boone, A., Etchevers, P., Habets, F., Noilhan, J., Braden, H., Cox, P.M., de Rosnay, P., Dickinson, R. E., Yang, Z.L., Dai, Y.J., Zeng, Q., Duan, Q., Koren, V., Schaake, S., Gedney, N., Gusev, Y.M., Nasonova, O.N., Kim, J., Kowalczyk, E.A., Shmakin, A.B., Smirnova, T.G., Verseghy, D., Wetzel, P. and Xue, Y. (2001) The representation of snow in land surface schemes: results from PILPS 2(d). *Journal of Hydrometeorology*, 2, 7–25.

Stieglitz, M., Déry, S.J., Romanovsky, V.E. and Osterkamp, T.E. (2003) The role of snow cover in the warming of Arctic permafrost. *Geophysical Research Letters*, 30(13), 1721. https://doi.org/10.1029/2003GL017337.

Vikhamar-Schuler, D., Edwards, J.M., Rooney, G. and Kristiansen, J. (2012) Evaluation of JULES multi-layer snow scheme for Norwegian snow conditions. *Geophysical Research Abstracts*, 14, EGU2012–EGU3725.

Vionnet, V., Brun, E., Morin, S., Boone, A., Faroux, S., Le Moigne, P., Martin, E. and Willemet, J.M. (2012) The detailed snowpack scheme Crocus and its implementation in SURFEX v7.2. *Geoscientific Model Development*, 5, 773–791. https://doi.org/10.5194/gmd-5-773-2012.

Walters, D.N., Best, M.J., Bushell, A.C., Copsey, D., Edwards, J.M., Falloon, P.D., Harris, C.M., Lock, A.P., Manners, J.C., Morcrette, C.J., Roberts, M.J., Stratton, R.A., Webster, S., Wilkinson, J.M., Willett, M.R., Boutle, I.A., Earnshaw, P.D., Hill, P.G., MacLachlan, C., Martin, G.M., Moufouma-Okia, W., Palmer, M.D., Petch, J.C., Rooney, G.G., Scaife, A.A. and Williams, K.D. (2011) The Met Office unified model global atmosphere 3.0/3.1 and JULES global land 3.0/3.1 configurations. *Geoscientific Model Development*, 4, 919–941. https://doi.org/10.5194/gmd-4-919-2011.

Webster, S., Brown, A.R., Jones, C.P. and Cameron, D.R. (2003) Improvements to the representation of orography in the Met Office Unified Model. *Quarterly Journal of the Royal Meteorological Society*, 129, 1989–2010.

Wiscombe, W.J. and Warren, S.G. (1980) A model for the spectral albedo of snow. I: Pure snow. *Journal of the Atmospheric Sciences*, 37, 2712–2733.

Yang, Y., Uddstrom, M., Revell, M., Andrews, P., Oliver, H., Turner, R. and Carey-Smith, T. (2011) Numerical simulations of effects of soil moisture and modification by mountains over New Zealand in summer. *Monthly Weather Review*, 139, 494–510.

Yang, Y., Uddstrom, M., Revell, M., Andrews, P. and Turner, R. (2012) Amplification of the impact of assimilating ATOVS radiances on simulated surface air temperatures over Canterbury by the Southern Alps, New Zealand. *Monthly Weather Review*, 140, 1367–1384.

Yang, Y., Uddstrom, M., Revell, M. and Moore, S. (2013) Soil moisture simulation by the JULES in New Zealand: verification and

sensitivity tests. *Meteorological Applications*, 21, 888–897. https://doi.org/10.1002/met.1426.

Yang, Y., Uddstrom, M., Revell, M., Moore, S. and Turner, R. (2017) Damaging southerly winds caused by barrier jets in the Cook Strait and Wellington Region of New Zealand. *Monthly Weather Review*, 145, 1203–1220. https://doi.org/10.1175/MWR-D-16-0159.1.

How to cite this article: Yang Y, Uddstrom M, Turner R, Revell M. Major factors affecting the snow simulations by the JULES in New Zealand. *Meteorol Appl*. 2020;27:e1837. https://doi.org/10.1002/met.1837